Mecánica Computacional Vol. XXIV
A. Larreteguy (Editor)
Buenos Aires, Argentina, Noviembre 2005

A COUPLED TIRE STRUCTURE-ACOUSTIC CAVITY MODEL

Leonardo R. Molisani[*] and Ricardo A. Burdisso[†]

[*] Office 25, Department of Mechanical Engineering
Universidad Nacional de Río Cuarto, Ruta Nac. 36 - Km. 601
CP 5800 Río Cuarto, Córdoba, Argentina
e-mail: lmolisani@ing.unrc.edu.ar, web page: http://www.unrc.edu.ar

[†] 153 Durham Hall, Department of Mechanical Engineering
Virginia Polytechnic Institute & State University,
Blacksburg, VA 24061, United States of America
e-mail: rburdiss@vt.edu, web page: http://www.val.me.vt.edu

Key words: acoustic cavity-tire structure interaction, resonance control techniques.

Abstract. *Recent experimental results have shown that the vibration induced by the tire air cavity resonance is transmitted into the vehicle cabin and may be responsible for significant interior noise. The tire acoustic cavity is excited by the road surface through the contact patch on the rotating tire. The effect of the cavity resonance is that results in significant forces developed at the vehicle's spindle, which in turn drives the vehicle's interior acoustic field. This tire-cavity interaction phenomenon is analytically investigated by modeling the fully coupled tire-cavity systems. The tire is modeled as an annular shell structure in contact with the road surface. The rotating contact patch or a harmonic point force is used as a forcing function in the coupled tire-cavity governing equation of motion. The contact patch is defined as a prescribed deformation that in turn is expanded in its Fourier components. The response of the tire is then separated into static and dynamic components. The coupled system of equations is then solved in closed form in order to obtain the tire acoustic and structural responses. The influence of the acoustic cavity resonance on the spindles forces is shown to be very important. Therefore, the tire cavity resonance effect must be reduced in order to control the tire contribution to the vehicle interior noise. The modeling and analysis of an approach to control the tire acoustic cavity resonances is investigated. The approach consists in the incorporation of secondary acoustic cavities to detune and damp out the main tire cavity resonance. The model is used to show that the secondary cavities are effective at suppressing the tire cavity resonance and thus the forces at the spindle.*

1 INTRODUCTION

The main aim of this work is to derive the model of the dynamic response of a deformed tire. The general steps in the development of the deformed tire model are shown in Figure 1 and it is based on the work by Molisani[1]. The region of the tire deformed due to the contact with the ground is assumed to be perfectly defined by the geometry of the problem. That is, the tire deforms from a circular sector to a flat surface called contact patch as shown in Figure 1(a). The contact patch imposes a prescribed deformation of the tire that needs to be defined. The size of this region (footprint) is completely defined by the static contact patch depth, $\bar{h}$. The prescribed deformation function in turn induces a static displacement field on the rest of the tire which is shown in Figure 1(b). This static displacement field is obtained by using the classical equations for the elastic shells. After the static displacement field is obtained, a harmonic motion of the contact patch around the equilibrium position, defined by the contact patch depth, is superimposed. This contact patch harmonic motion produces a dynamic displacement field due to the inertia properties of the elastic shell. A representation of the dynamic displacement is shown in Figure 1(c). Thus, the formulation of the deformed tire case involves the modeling of the prescribed, static, and dynamic displacement fields.

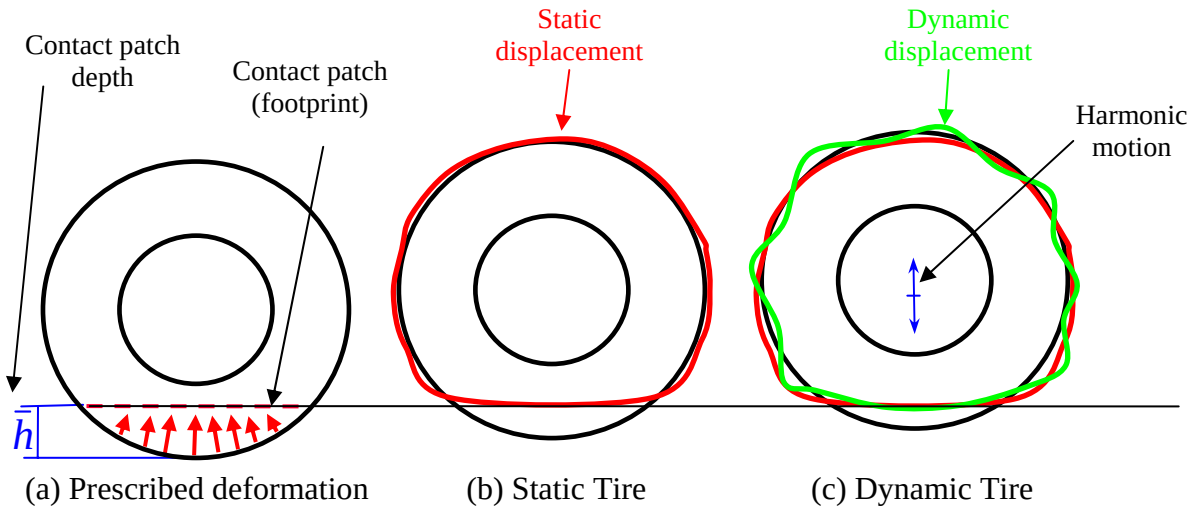

Figure 1: Schematic of the contact patch modelling.

2 PRESCRIBED DEFORMATION

The prescribed displacement is assumed symmetric with respect to $d(x,\theta)$. The prescribed displacement function is assumed to be affecting only the radial direction, i.e. a point on the tire in contact with the ground moves along the radial direction. This modeling assumption is

shown in Figure 2 and it is critical for the next step in finding the static displacement.

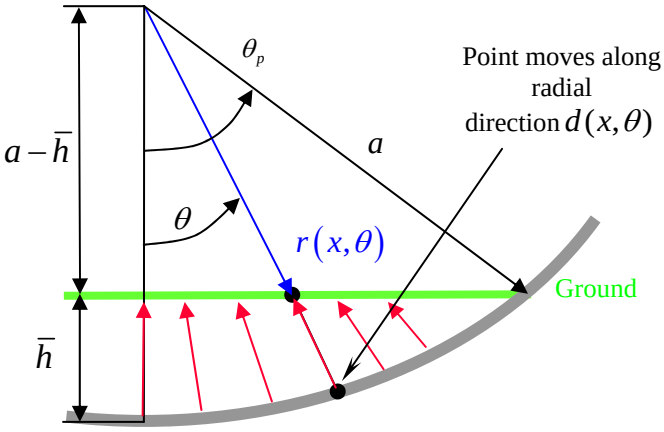

Figure 2: Contact patch definition at $x=L_T/2$.

The domain of definition for the "contact patch" is given by

$$D=\left\{x/x\in\left[0,L_T\right]\wedge\theta/\theta\in\left[\theta_p\left(\bar{h}\right),-\theta_p\left(\bar{h}\right)\right]\right\} \tag{1}$$

where L_T is tire width. The prescribed displacement function is then given by

$$d\left(x,\theta\right)=\left\{\left[\bar{h}-a\right]\sec\left(\theta\right)-a\right\}\left[H\left(x-L_T\right)-H\left(x-0\right)\right] \tag{2}$$

where $H(.)$ is the Heaviside's unit step function.

3 STATIC DISPLACEMENT

The prescribed deformation function *d(x,θ)* induces a static deformation in the elastic shell as shown in Figure 1(b). In order to find the static displacement, the prescribed deformation is approximated by the eigenfunctions of the shell. The selection of these functions simplifies the approach because they satisfy the shell equations and the simply supported boundary conditions (shear diaphragms[2]). That is,

$$w^S\left(x,\theta\right)=\sum_{m=1}^{M}\sum_{n=0}^{N}W_{mn}^{(3)}\sin\left(\frac{m\pi}{L_T}x\right)\cos\left(n\theta\right) \tag{3}$$

Note that the static displacement in (3) is written only for the radial component of the displacement field. The other two components of the displacement field is defined later using the elasticity equations[1]. The aim now is to solve for the unknown modal amplitude $W_{mn}^{(3)}$. To

this end, the radial component of the static displacement in (3) is forced to match the prescribed displacement (2) over the contact patch sector. This matching yields a linear system of equations given by

$$\int_{O}^{L}\int_{-\theta_p}^{\theta_p} d(x,\theta)\sin\left(s\frac{\pi}{L_T}x\right)\cos(r\theta)\,a\,d\theta dx = \\ = \int_{O}^{L}\int_{-\theta_p}^{\theta_p}\left[\sum_{m}^{M}\sum_{n}^{N} W_{mn}^{(3)}\sin\left(\frac{m\pi}{L_T}x\right)\cos(n\theta)\sin\left(\frac{s\pi}{L_T}x\right)\cos(r\theta)\right] a d\theta dx \tag{4}$$

Terms are included in the series until the contact patch is well approximated and therefore the match is satisfied. In Figure 3, the radial static displacement field w^S is shown. The upper figure represents the complete tire shell. The lower figure shows the contact patch region in detail. Therefore, the three-dimensional form of the contact patch modeled in this effort can be appreciated.

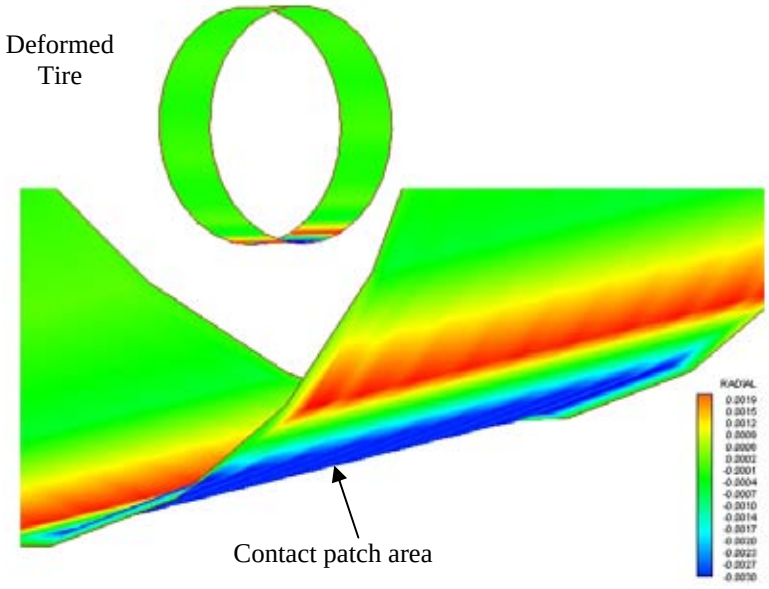

Figure 3: Radial displacement field w^S [m] for tire.

In Figure 4, the static displacement predicted by the model is compared with experimental data collected by Yamauchi and Akiyoshi[3] for a tire size 195/65 R15. This figure shows the radial displacement of the "deformed tire", w^s, and the prescribed displacement function, $d(x,\theta)$, around the tire in the azimuth direction at the center line $x=L_T/2$. The radial displacement, w^s, matches the contact patch very well. However, a very significant oscillation is observed and it is due to the (1,8) mode. In order to compare the experimental data, a moving average of the static displacement away from the contact patch is also plotted (blue line). The average curve shows similar trend as the experiments. This suggests that the model

overemphasizes the high order mode component not observed experimentally. Note that this (1,8) mode component associated to the oscillation will not contribute to the spindle forces because it does not correspond to a "beam" mode[1] with *n=1*. The predicted results shown in this figure are in relatively good agreement with the measured results in the contact patch area.

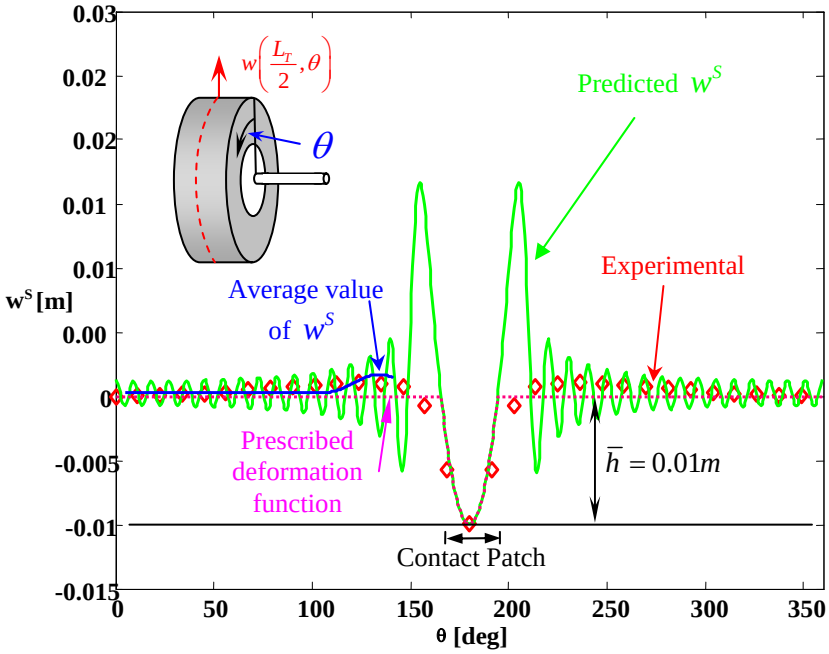

Figure 4: Comparison of predicted and experimental radial displacement for a tire size 195/65 R15 (Exp. Data from Yamauchi and Akiyoshi[3]).

The formulation up to this point allows finding the radial displacement component, w^s. That is the radial coefficient of the static displacement field as defined in equation (3). The other two components, i.e. axial u^s and the tangential v^s are determined by using the equation of the elastic shell. Complete details can be found in the work of Molisani[1].

4 DYNAMIC DISPLACEMENT

The dynamic motion of the system is assumed to be produced by a harmonic vertical motion of the tire as shown in Figure 1(c). The vertical motion of the tire translates into a time variation of the contact patch depth that can be expressed as

$$h(t) = \bar{h} + \varepsilon\, e^{i\omega t} \tag{5}$$

where ε is the amplitude of the tire harmonic motion. The response spectrum for constant amplitude of the vertical motion ε can be determined from the road characteristic, i.e

roughness of the road. The displacement induced now by the time dependant contact patch depth, *h(t)*, oscillating with radial frequency ω induces inertial forces in the tire shell.

The inertial effects will produce a dynamic response that needs to be superimposed to the static deformation. To solve for the time-dependant displacement vector, small motion are assumed i.e. $\varepsilon \ll \bar{h}$. Therefore, $\bar{h}$ is substituted by *h(t)* in the system of equations of eq. (4), and linearized with respect to *h(t)* by using Taylor's series expansion evaluated around the equilibrium position $\bar{h}$. Thus, the complete static displacement field and the time-dependant part are fully defined, i.e. $\{u^s, v^s, w^s\}^T = \{\bar{u}^s, \bar{v}^s, \bar{w}^s\}^T + \{\tilde{u}^s, \tilde{v}^s, \tilde{w}^s\}^T$. It is important to note that it was found that the axial and tangential time variation displacement components can be neglected since their contribution to the response is insignificant[1].

The dynamic response due to the oscillating component of the static displacement field, $\{\tilde{u}^s, \tilde{v}^s, \tilde{w}^s\}^T$, can now be determined. Applying the shell Donnell-Mushtari operator to the total displacement vector $\{u^t\}$ as follow

$$\left(\left[L_c\right] - \Omega^2\left[I\right]\right)\begin{Bmatrix} u^t \\ v^t \\ w^t \end{Bmatrix} = \{0\} \tag{6}$$

where the total displacement vector is the contribution of the dynamic displacement due to the shell inertia and the time-dependant part of the static displacement due to the contact patch oscillation around $\bar{h}$. The dynamic response of the "deformed tire" model is then used to compute the forces at the spindle.

5 COUPLED STRUCTURAL-ACOUSTIC PROBLEM

The cavity-structure interaction problem is now solved. Figure 5 illustrates the problem of a structure and the interior acoustic pressure. Here a brief description of the coupled problem will be presented for a general understanding of the solution approach.

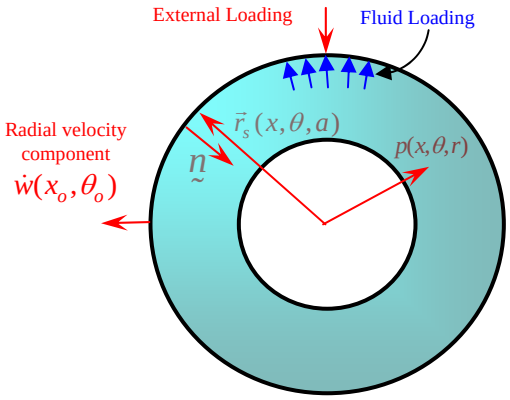

Figure 5: Structure radiating into an enclosed volume.

The approach to solve the coupled problem is to include in the equation of motion of the tire the force due to the interior pressure, i.e. fluid loading. However, the fluid forces depend on the velocity response of the structure which leads to a fluid feedback problem. The equation of motion of the system including the fluid loading is written as

$$\left(\left[L_c\right]-\Omega^2\left[I\right]\right)\begin{Bmatrix}u\\v\\w\end{Bmatrix}=\begin{Bmatrix}f_u\\f_v\\f_w\end{Bmatrix}-\begin{Bmatrix}0\\0\\p(x,\theta,a)\end{Bmatrix} \tag{7}$$

The forcing function $\{f_u, f_v, f_w\}^T$ in equation (7) is the external load. The external load is the contact patch forcing function for the "deformed tire" model. The model also permits to change the forcing function to excite the undeformed or "free tire", i.e. a harmonic force[4]. The last vector in (7) represents the acoustic pressure acting on the tire[5], given by the following equation

$$p(x,\theta,a)=\varepsilon_{\Im}\int_0^{L_T}\int_0^{2\pi} i\omega\rho\dot{w}(x_o,\theta_o)G(x,\theta,a|x_o,\theta_o,a)\;a\;\mathrm{d}\theta_o\;dx_o \tag{8}$$

where $\dot{w}(x_o,\theta_o)$ is the radial component of the shell velocity response, ρ is the air density, $\varepsilon_{\Im}$ is the integration constant related to de Dirac delta, and $G(x,\theta,r|x_o,\theta_o,a)$ is the Green's function[1].

To demonstrate the capability of the model, the analytical tire model was validated against experimental results[1]. The test cases were a free tire driven by a point force (referred as undeformed case) and the deformed tire driven by the contact patch forcing function. Figure 6 shows both cases (a) undeformed and (b) deformed tire. In each plot, there are three curves corresponding to the in vacuo model (without the effect of the tire cavity) in red dotted line, the coupled model in blue solid line, and the experimental results from a test measurement performed by Yamauchi and Akiyoshi[3] in a green dash-dotted line. The results from this simple analytical model show qualitatively similar trends as the experimental observation, i.e. blue line for the coupled case and green line for experimental results. The green line corresponding to the experimental data shows also the presence of the rigid body motion, which is not accounted for the model. The dynamic of the tire structure is clearly represented and the effect of the tire acoustic cavity is very well predicted in both cases i.e. undeformed and deformed tire.

The model was then used to predict the forces at the spindle of the car for the undeformed and deformed tire cases. In both cases, the force predicted by the model shows a significant effect due to the tire acoustic cavity resonance[1].

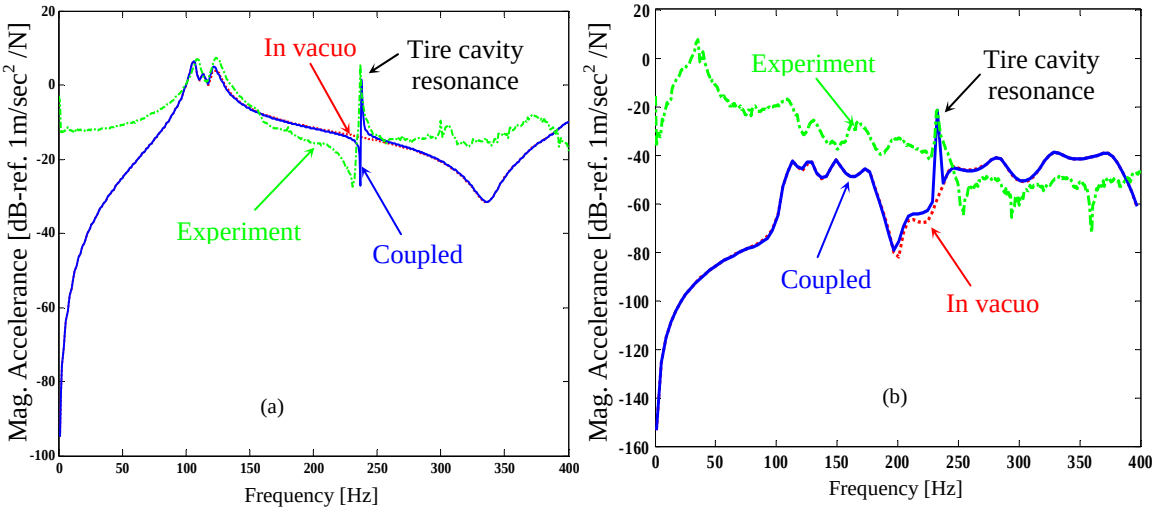

Figure 6: Magnitude of the Point Accelerance (a) the free and (b) deformed tire model measured at the wheel center.

6 CAVITY ACOUSTIC CONTROL

The influence of the acoustic cavity dynamics results in a sharp increase of the spindle forces around the tire cavity resonance. Therefore, the tire cavity resonance effect must be reduced in order to control the tire contribution to the structural born noise. The approach proposed here is the incorporation of secondary acoustic cavities to detune and damp out the main tire cavity resonance. The secondary cavity control approach is similar to the concept of Dynamic Vibration Absorber (DVA) used in structures[6]. The DVA concept is applied to detune the tire acoustic cavity resonance by using secondary cavities, i.e. the (0,1,0) acoustic mode[4]. The effect of the rotation of the tire is accounted by using two secondary cavities placed 90^o apart from each other.

The tire main and secondary cavities are interconnected by openings which are referred here as the "coupling interfaces". To introduce damping in the system, sound absorptive screens such as wiremesh, perforate plates, and so forth can be implemented at these interfaces. The model is illustrated in Figure 7 and involves first separating the secondary cavities from the tire cavity. Then, the effect of the secondary cavities on the tire cavity is considered or modeled as an additional moving boundary in the formulation, i.e. in addition to the elastic shell motion. For simplicity and without loss of generality, the secondary cavities are modeled as a constant cross section straight waveguide (tube) as shown in Figures 7. The size of the tube cross section is assumed much smaller than the acoustic wavelength. Since for typical tires the acoustic resonance (0,1,0) is at few hundred Hertz, this assumption is valid and implies that the motion of the boundary at the coupling interfaces can be modeled as a piston sources with unknown normal velocity $\dot{z}_j$ with $j=1,2$. The couple response of the tire structure and acoustic cavity (tire and secondary cavities) is again the solution of the system (7).

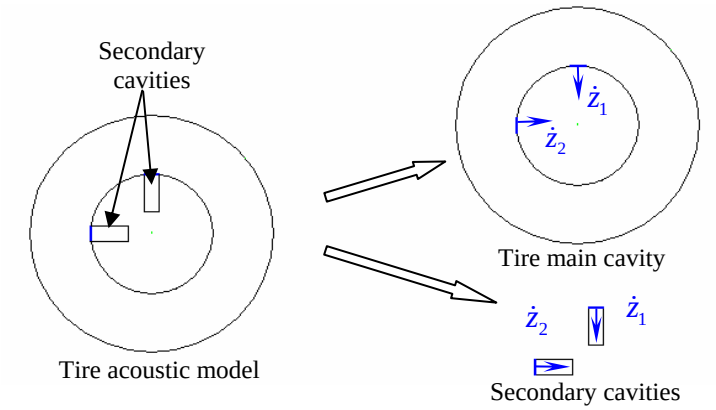

Figure 7: Tire and secondary cavities acoustic modelling.

The expression for the acoustic pressure $p(x,\theta,a)$ has now to include the effect of the secondary cavities, i.e. piston sources.

$$p(x,\theta,a) = \int_0^{L_T}\int_0^{2\pi} i\omega\rho\dot{w}(x_o,\theta_o)G(x,\theta,a|x_o,\theta_o,a)\, a\, \mathrm{d}\theta_o\, dx_o - \sum_{j=1}^{2} S_j G(x,\theta,a|x_o^{(j)},\theta_o^{(j)},b) i\omega\rho\dot{z}_j \qquad (9)$$

To illustrate the performance of the control approach, Figure 8 shows the magnitude of the vertical force at the spindle for (a) the free tire model and (b) the deformed tire model.

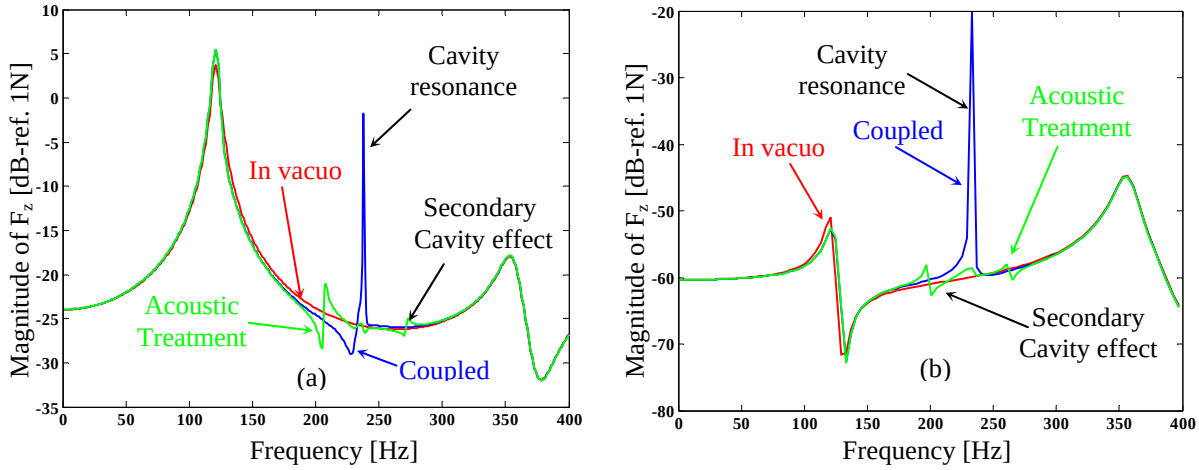

Figure 8: Magnitude of the vertical force at the spindle (a) the free tire model and (b) deformed tire model.

The figure shows the cases for the in vacuo model (red line), the coupled model without the secondary cavities (blue line), and the coupled model with the secondary cavities (green line). From the results in the figure, it can be observed that the concept is very effective at suppressing the acoustic cavity resonance for the undeformed and deformed tire cases. The secondary cavities successfully achieve the acoustic resonance control.

7 CONCLUSION

A model for the coupled tire-cavity was developed and validated against experimental results. The model shows that the acoustic cavity resonance has a very dominant effect in the response of the tire. In addition, the model was also used to investigate a control approach consisting on adding secondary cavities to suppress the adverse effects of the acoustic cavity in the tire response. This method is effective and can be easily implemented in practice.

8 ACKNOWLEDGMENTS

The authors want to express gratitude to Hiroshi Yamauchi for his contribution with experimental data and his interest related to this work.

9 REFERENCES

[1] L. Molisani, *A Coupled Tire-structure Acoustic Cavity Model*, Doctoral Dissertation, Virginia Tech, (2004).

[2] A. Leissa, *Vibration of Shells*, Acoustical Society of America, (1993).

[3] H. Yamauchi and Y. Akiyoshi, "Theoretical Analysis of tire Acoustic Cavity Noise and Proposal of Improvement Techniques", *Society of Automotive Engineers of Japan, Inc. and Elsevier Science (JSAE),* Review 23, pp 89-94 (2002).

[4] L. Molisani, R. A. Burdisso, and D. Tsihlas, "A Coupled Tire Structure/Acoustic Cavity Model", *Int. J. of Solids and Structures*, 40, pp 5125-5138 (2003).

[5] F. Fahy, *Sound and Structural Vibration*, Academic Press, (2000).

[6] L. Meirovitch, *Fundamentals of Vibrations*, McGraw-Hill, (2001).